

# Solid state reaction and formation of nano-phase composite hydrogen storage alloy by mechanical alloying of $\text{MmNi}_{3.5}(\text{CoMnAl})_{1.5}$ and Mg

Y. GAO, M. Q. ZENG, B. L. LI, M. ZHU\*

*College of Mechanical Engineering, South China University of Technology,  
Guangzhou 510641, People's Republic of China*  
E-mail: memzhu@scut.edu.cn

C. Y. CHUNG

*Department of Physics and Materials Science, City University of Hong Kong,  
Kowloon, Hong Kong*

In this work  $\text{MmNi}_{3.5}(\text{CoMnAl})_{1.5}$  and Mg were mechanically alloyed to prepare composite hydrogen storage alloys. The microstructural variation of the alloy resulted from the mechanical alloying was characterized by X-ray diffraction, SEM and TEM analysis. It was found that solid state reaction occurred between  $\text{MmNi}_{3.5}(\text{CoMnAl})_{1.5}$  and Mg components, resulting in  $\text{Mm}_2\text{Mg}_{17}$  phase formation. The alloy obtained by ball milling contains homogeneously distributed Mg,  $\text{MmNi}_{3.5}(\text{CoMnAl})_{1.5}$  and  $\text{Mm}_2\text{Mg}_{17}$  phases of nanometer size. It was also found that  $\text{Mg}_2\text{Ni}$  was formed after the mechanically alloyed samples were annealed. The mechanism of the reaction has been proposed based on the estimation of the heat of formation using Miedema's theory and is in accordance with the experiment result of lattice constant measurement of ball milled sample and its structure variation during annealing. © 2003 Kluwer Academic Publishers

## 1. Introduction

It has well been established that nanocrystalline materials exhibit many unique properties such as very high diffusion rates, high chemical activity and high strength [1]. The behavior of hydrogen in nanocrystalline metals is also different, in some aspects, to that in conventional metals. It was found, for instance, that there was an increase in the solubility of hydrogen in nanocrystalline Pd prepared by gas condensation [2]. In the past years, a lot of effort has been made to fabricate nanocrystalline hydrogen storage alloys and to investigate the relationship among their composition, microstructure and properties [3]. Mechanical alloying (MA) was, in most of the cases, used to synthesize nanocrystalline hydrogen storage alloys for it is a convenient and efficient way of preparing materials with metastable microstructure such as amorphous, nanocrystalline and supersaturated solid solution in various materials systems. As having been demonstrated in many hydrogen storage alloys, such as TiFe [4],  $\text{LaNi}_5$  [5],  $\text{Mg}_2\text{Ni}$  [6] and  $\text{MgNi}$  [7], the activity and kinetics of alloys prepared by MA were greatly improved.

Nano-phase composite hydrogen storage alloys prepared by MA have been extensively investigated in recent years. This is because that superior comprehensive properties, including hydrogen storage capacity, activity, kinetics and so on, could hardly be achieved in any

of the  $\text{AB}_5$ ,  $\text{AB}_2$ , AB type and Mg base alloys developed so far. For instance, Mg base alloy has large hydrogen storage capacity, but it reacts with  $\text{H}_2$  at temperature over  $300^\circ\text{C}$  and its hydrogen absorption/desorption kinetics is poor. In contrast,  $\text{LaNi}_5$  alloy system exhibits suitable hydriding reaction temperature and good kinetics, but its hydrogen storage capacity is small. It was considered that good hydrogen storage properties could be gained by forming composite alloy constituted of different hydrogen storage alloys and a lot of study has been made [8–14]. Improvement of hydrogen absorption properties such as reaction rate, reaction temperature and activity was observed in many previous works. It has been found that interaction existed between different phases and high density of boundaries is beneficial to the improvement of properties of composite hydrogen storage alloys. Therefore, preparation of nanocomposite is of significant.

It is well known that MA results in complicated microstructure variation such as microstructure refining, metastable phase formation and solid state reaction (SSR) [15]. In a previous paper [14] we reported the preparation of  $\text{Mg}/\text{MmNi}_{3.5}(\text{CoMnAl})_{1.5}$  composite hydrogen storage alloy and apparent improvement of hydrogen absorption properties. However,  $\text{Mm}_2\text{Mg}_{17}$  phase was found to form after milling, which indicated the occurrence of SSR. In this article X-ray, SEM and

\*Author to whom all correspondence should be addressed.

TEM analysis were used to clarify the microstructure evolution process and mechanism of SSR in the MA of Mg and  $\text{MmNi}_{3.5}(\text{CoMnAl})_{1.5}$ .

## 2. Experiment procedure

$\text{MmNi}_{3.5}(\text{CoMnAl})_{1.5}$  (briefly denoted as  $\text{MmM}_5$  here after) alloy was prepared by induction melting under protection of pure argon. The ingot was crushed to powder with size less than 1 mm. The Mg used was commercial powder with purity of 99.8% and size of 200 mesh.  $\text{MmM}_5$ -Mg powder mixtures with composition of  $\text{MmM}_5$ -5%Mg,  $\text{MmM}_5$ -10%Mg,  $\text{MmM}_5$ -30%Mg and  $\text{MmM}_5$ -50%Mg (wt pct) were put together with hardened steel balls into stainless steel vial and milled in a Fritsch P-5 planetary ball mill with rotating speed of 150 rpm. The weight ratio of ball to powder was 10:1. The ball milling process was carried out under the protection of pure argon. X-ray diffraction analysis, SEM and TEM analysis were used to investigate the structure variation of the milled sample. The X-ray diffractometer used was Rigaku D/MAX-RC with  $\text{Cu K}\alpha$  radiation. The SEM and TEM used were Hitachi S-550 and Philips CM-30 respectively. Composition was analysed by an EDX accessory attached to SEM. The preparation of specimen for TEM observation was similar to that described before [16].

## 3. Results and discussions

Fig. 1a, b and c are secondary electron images of  $\text{MmM}_5$ -10 wt%Mg powder obtained by milling for 0.5, 2 and 20 hr respectively. Fig. 1d is an enlarged image of Fig. 1c. EDX analysis proved that the bright particle in Fig. 1a corresponded to  $\text{MmM}_5$  component. It can be seen that the  $\text{MmM}_5$  component was gradually refined as milling proceeded. The typical morphology of powder obtained by long time milling is shown in Fig. 1c. It is seen that the  $\text{MmM}_5$  component was very fine and aggregated together forming composite particles consisted of granules. EDX result indicated that the average composition of the particles agreed with the nominal composition of powder mixture. The morphology of powder mixture obtained by 20 hr of milling, as shown in Fig. 1c, was not apparently changed in the further milling process. This means that a steady state of microstructure was reached after about 20 hr of milling. The formation of the microstructure mentioned above should be related to the intrinsic properties of the two constituents of the powder mixture. The  $\text{MmM}_5$  phase is a very brittle intermetallic compound and pure Mg is much softer compared with  $\text{MmM}_5$ . They constitute a typical brittle/tough system. Previously, it was demonstrated in the ball milling of brittle/tough system [17] that the brittle component was rapidly fragmented, while deformation, fracture and cold welding took place in tough component. The

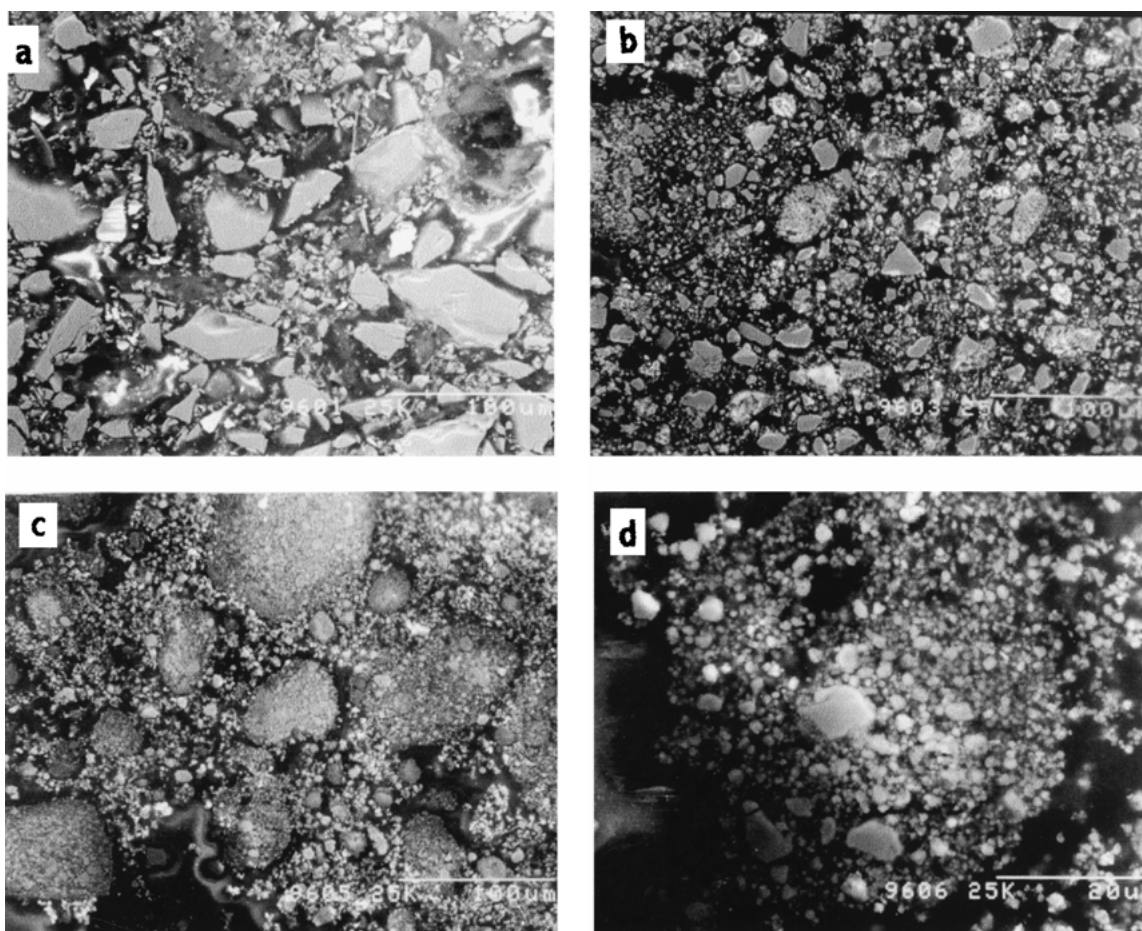


Figure 1 SEM micrographs of  $\text{MmM}_5$ -10 wt%Mg powder mixture milled for different time: (a) 0.5 hr, (b) 2 hr, (c) 20 hr, and (d) higher magnification of (c).

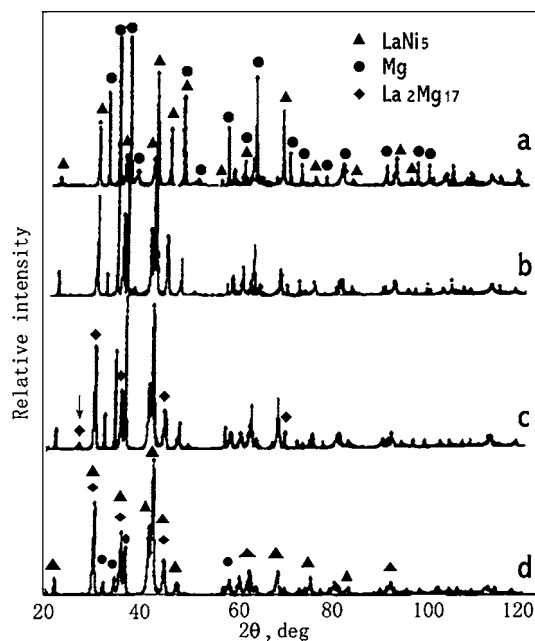


Figure 2 X-ray diffractograms of MmM<sub>5</sub>-30 wt%Mg powder obtained by milling for different times: (a) 0.5 hr, (b) 2 hr, (c) 8 hr, and (d) 20 hr.

fragmented brittle component was embedded into lamella of tough component. As the milling prolonged, the microstructure was refined and the two components blended together homogeneously and aggregates of granules were formed. Thus, microstructure of very fine MmM<sub>5</sub> particles bonded by Mg, as is shown in Fig. 1c, was obtained after long time milling. It is evident that this kind of microstructure contains very high ratio of interfaces.

More details of microstructure characteristics can be found by X-ray diffraction and TEM analysis. The X-ray diffractograms a, b, c and d placed in Fig. 2 were obtained in sample with composition of MmM<sub>5</sub>-30 wt%Mg milled for 0.5, 2, 8, and 20 hr respectively. It was found that the X-ray diffractograms were not apparently changed in milling process beyond 20 hr. It can be seen that diffraction peaks of both MmM<sub>5</sub> and Mg components broadened as milling proceeded, which indicated the reduction of grain size of both and existence of internal strain. The estimation of grain size, from peak broadening by the method described in reference [18], shows that the grain size of both MmM<sub>5</sub> and Mg was greatly reduced after 20 hr of milling. For example, the grain size of MmM<sub>5</sub> and Mg reached 23 and 16 nm respectively after 20 hr of milling of MmM<sub>5</sub>-30 wt%Mg mixture. The results described above proved that nanocrystalline composite with average grain size of 20 nm was formed in the MmM<sub>5</sub>-Mg system after about 20 hr of milling.

However, Mg content of powder mixture has apparent influence on grain size of MmM<sub>5</sub> component. The dependence of grain size of MmM<sub>5</sub> phase on milling time for the samples of different Mg contents is shown in Fig. 3a and b. It has been found that the change of grain size on milling time can be described by following formula [19]:

$$D = At^{-b} \quad (1)$$

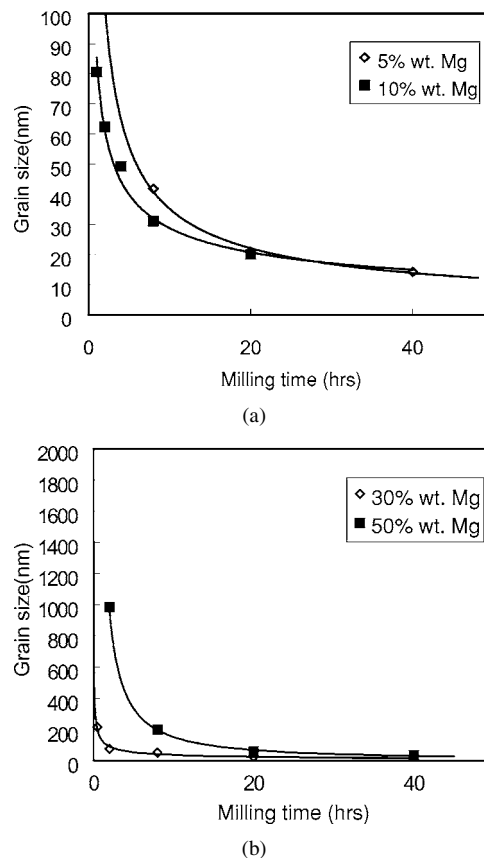


Figure 3 The dependence of grain size of MmM<sub>5</sub> phase on milling time for the sample of different Mg contents: (a) MmM<sub>5</sub>-5%Mg and MmM<sub>5</sub>-10%Mg and (b) MmM<sub>5</sub>-30%Mg and MmM<sub>5</sub>-50%Mg.

where  $D$  is grain size,  $t$  is milling time,  $A$  and  $b$  are constant. For the milling of single component,  $b$  is  $2/3$ . The curves of grain size of MmM<sub>5</sub> and Mg phase on milling time were fitted using Equation 1 and the results obtained were listed in Table I. It can be seen that  $b$  value for MmM<sub>5</sub> phase is very close to  $2/3$  when Mg content in powder mixture is low (5 wt% Mg), while  $b$  value for Mg phase is very close to  $2/3$  when Mg content in powder mixture is high (50 wt% Mg). For other compositions, the  $b$  value is deviated from  $2/3$ . This is because that the powder mixture behaves like MmNi<sub>5</sub> or Mg single phase system when Mg content is low or high respectively. The grain size of MmM<sub>5</sub> phase obtained by 20 hr of milling in powder mixture of different Mg content is given in Fig. 4. It can be seen that the grain size is larger when Mg content is high. These results reveal that the existence of Mg influences the refining of MmM<sub>5</sub> and the existence of MmNi<sub>5</sub> influences the refining of Mg. This is probably owing to the

TABLE I The value of  $A$  and  $b$  for MmM<sub>5</sub> and Mg phase for samples of different Mg contents

Composition of samples	Fitting result for MmM <sub>5</sub> phase		Fitting result for Mg phase	
	$A$	$b$	$A$	$b$
MmM <sub>5</sub> -5% wt Mg	164.36	0.6688		
MmM <sub>5</sub> -10% wt Mg	78.995	0.4315		
MmM <sub>5</sub> -30% wt Mg	135.05	0.5624	77.023	0.3798
MmM <sub>5</sub> -50% wt Mg	2126.5	1.1469	84.182	0.679

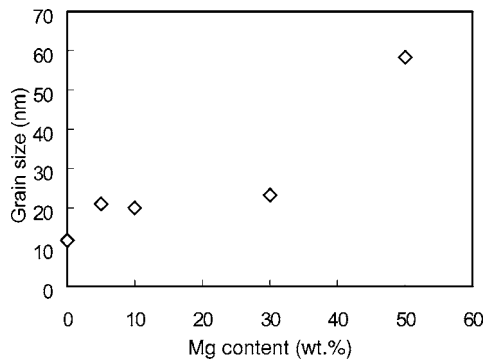


Figure 4 Dependence of average grain size of MmM<sub>5</sub> component on Mg content in MmM<sub>5</sub>-Mg powder mixture with different Mg contents milled for 20 hr.

fact that the stress of collision applied to MmM<sub>5</sub> component was reduced with the increasing of Mg content since the MmM<sub>5</sub> particles were embedded into Mg as described before. It was likely that Mg acted as a buffer to the impact on MmM<sub>5</sub> in the milling.

It can be observed in Fig. 2 that the relative intensity of the diffraction peaks of Mg reduces comparing with that of MmM<sub>5</sub> as milling proceeded. Meanwhile, as shown in Fig. 2c, the relative intensity of some diffraction peaks, as indicated by “◆”, increased and a new peak, as indicated by the arrow “↓”, appeared. The

indexing proved that the newly appeared peak corresponded to the reflection of La<sub>2</sub>Mg<sub>17</sub> phase (Considering that mish metal was used in this work, the La<sub>2</sub>Mg<sub>17</sub> phase was actually Mm<sub>2</sub>Mg<sub>17</sub> phase. We denote it as Mm<sub>2</sub>Mg<sub>17</sub> in this paper). Those peaks indicated by “◆” can be indexed as the reflection of both MmM<sub>5</sub> and Mm<sub>2</sub>Mg<sub>17</sub> phases. However, comparing with diffraction peak of MmNi<sub>5</sub> phase in Fig. 2a, in which only MmNi<sub>5</sub> and Mg phase existed, the relative intensity of those peaks indicated by “◆” increased. Therefore, the intensity increase was likely owing to the superposition of MmNi<sub>5</sub> and Mm<sub>2</sub>Mg<sub>17</sub> phases. This result means that Mm<sub>2</sub>Mg<sub>17</sub> was formed by SSR between MmM<sub>5</sub> and Mg in the milling process. The peak indicated by the arrow can hardly be observed in the diffractogram of 20 hr milled sample. This is because the grain size was refined to 10–20 nm and high density of defect was created in the alloy. That weak peak of Mm<sub>2</sub>Mg<sub>17</sub> diminished due to strong background scattering. Actually, the diffraction of Mm<sub>2</sub>Mg<sub>17</sub> can be clearly observed in the electron diffraction pattern, given in Fig. 5, of 20 hr milled sample. In order to clarify the microstructure of the mechanically alloyed MmM<sub>5</sub>/Mg in more detail, TEM observation was made on the as milled powder. Fig. 5a and b show the morphology and corresponding electron diffraction

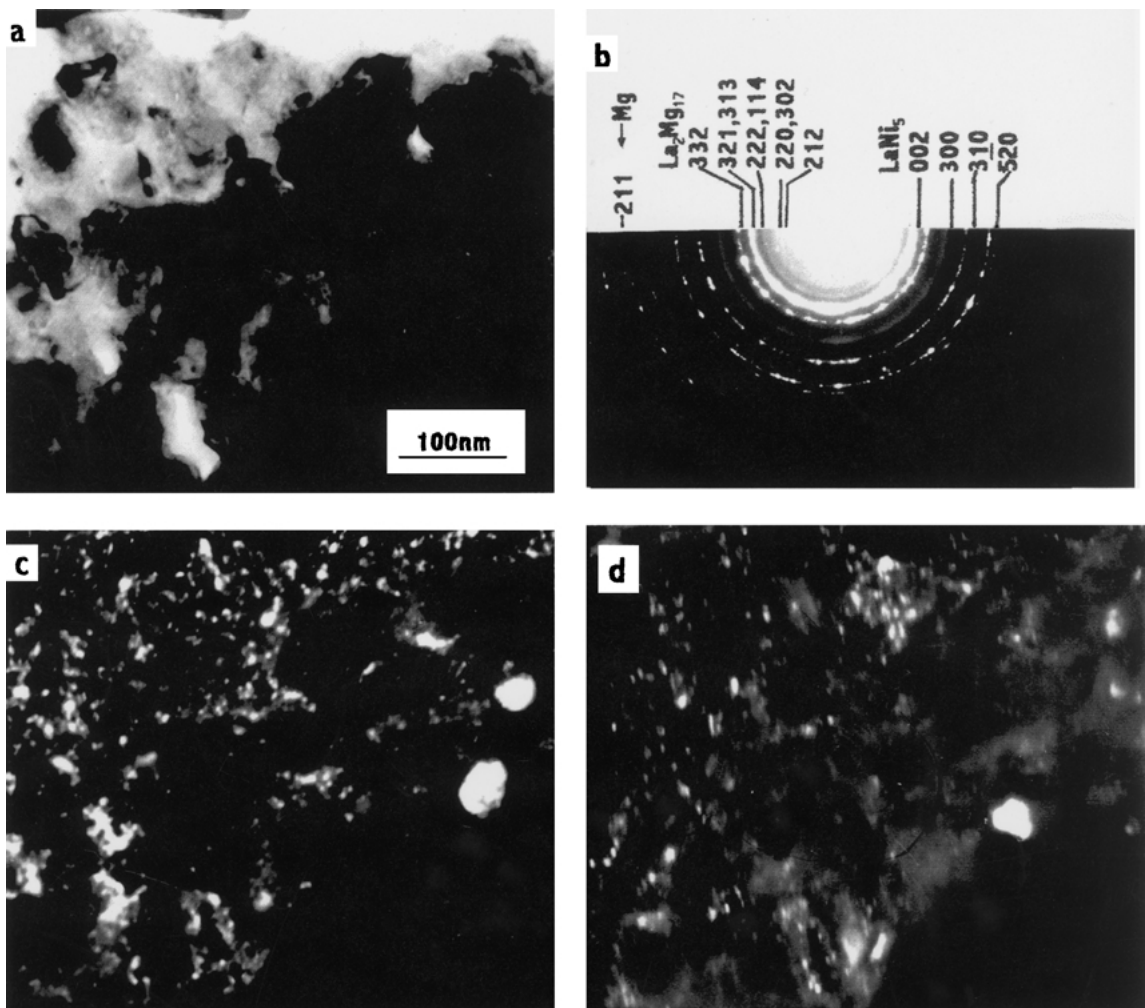
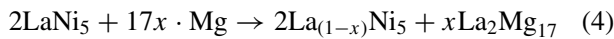
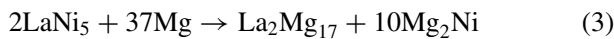
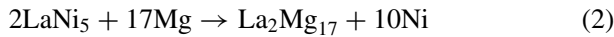


Figure 5 Morphology and electron diffraction pattern of MmM<sub>5</sub>-30%Mg specimen obtained by milling for 20 hr: (a) BF, (b) electron diffraction pattern, (c) DF imaged by 222 reflection of La<sub>2</sub>Mg<sub>17</sub>, and (d) DF imaged by 300 reflection of MmM<sub>5</sub>.

pattern of MmM<sub>5</sub>-30%Mg specimen obtained by milling for 20 hr. The indexing of the diffraction pattern proved that the constituent phases are MmNi<sub>5</sub>, Mg and Mm<sub>2</sub>Mg<sub>17</sub>. This result coincidences with the X-ray diffraction analysis described before. Fig. 5c and d are dark field images formed by 222 reflection of Mm<sub>2</sub>Mg<sub>17</sub> phase and 300 reflection of MmM<sub>5</sub> phase respectively (a section of diffraction hollow was circled by objective aperture to make dark field image). They clearly show that the constituent phases are homogeneously distributed and their size is about 10–20 nm, which is in agreement with the result deduced from X-ray diffraction analysis. In this sense it is considered that a nano-phase composite has been obtained.

SSR initiated by MA has been reported in many systems [20, 21]. It is believed that large strain and high interfacial energy induced by MA trigger the reaction in the fresh interface created by MA. The formation of Mm<sub>2</sub>Mg<sub>17</sub> phase after milling meant that SSR between MmM<sub>5</sub> and Mg took place. There are, at least, three possible reactions, as given below, in MmM<sub>5</sub>-Mg system (For simplify, we use La to replace mish metal Mm in the following calculation).



The enthalpy of formation,  $\Delta H$ , of LaNi<sub>5</sub> and Mg<sub>2</sub>Ni are –126 KJ/mol and –39 KJ/mol respectively, which was obtained from the data experimentally measured [22]. Since the  $\Delta H$  value of La<sub>2</sub>Mg<sub>17</sub> and La<sub>(1-x)</sub>Ni<sub>5</sub> was not found in literature, Miedema's empirical equation [22], as given in Equation 5, was used to calculate them and they are –133 JK/mol and –79.46 (for  $x = 0.05$ ) respectively.

$$\Delta H = c_A f_B^A \cdot \frac{V_A^{2/3}}{(n_{ws}^{-1/3})_{av}} [P(\Delta\phi^*)^2 + Q(\Delta n_{ws}^{1/3})^2 - R^*] \quad (5)$$

Then, we have the enthalpies of reaction for (2), (3) and (4) which are 172.5, –217 and –18.6 ( $x = 0.05$ ) KJ/mol respectively. Apparently, reaction (2) is impossible to take place for its positive enthalpy of reaction. It was also proved that no Ni, which would appear if reaction (2) occurred, was observed in X-ray diffraction and TEM analysis. As conjectured from enthalpy value, it is possible that both reaction (3) and (4) happen in milling process. If reaction (3) took place Mg<sub>2</sub>Ni phase should be observed. Although Mg<sub>2</sub>Ni phase was not observed in X-ray diffraction and TEM analysis in the as milled sample, there was possibility that the formed Mg<sub>2</sub>Ni phase was transformed into amorphous state during milling. This consideration was further supported by experiment evidence. As shown in Fig. 6, reflection peaks of Mg<sub>2</sub>Ni phase appeared in the sample annealed at 673 K after 20 hr of milling (a), but there is no diffraction peaks of Mg<sub>2</sub>Ni phase in the sample annealed at the same condition after milling for 0.5 hr (b). Therefore it was likely that reaction (2) did take place.

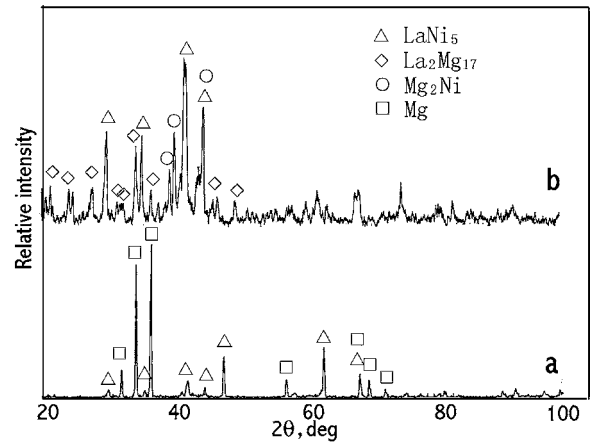


Figure 6 X-ray diffractograms of MmM<sub>5</sub>-30%Mg powder annealed at 673 K for 0.5 hr after milled for 0.5 hr (a) and 20 hr (b).

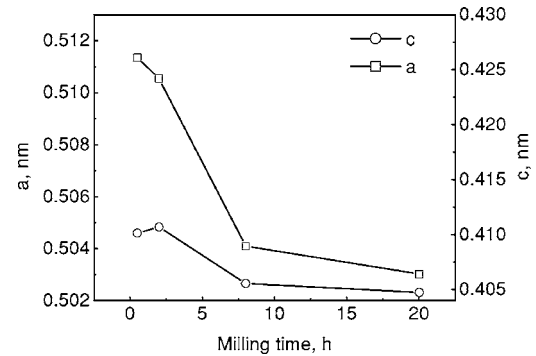


Figure 7 The dependence of lattice constant of MmNi<sub>5</sub> phase on time of milling in MmM<sub>5</sub>-30%Mg powder mixture.

With respect to reaction (3), if it took place, some of La atoms in LaNi<sub>5</sub> phase should be caught by Mg to form La<sub>2</sub>Mg<sub>17</sub> phase. This should cause the decrease of lattice constant of LaNi<sub>5</sub> phase for the radius of La atom, which is 0.187 nm, is larger than that of Ni, which is 0.125 nm. Thus, the change of lattice constant of the LaNi<sub>5</sub> phase in accordance with time of milling was measured and the result was given in Fig 7. It shows that the lattice constant reduced as the milling time increased. Therefore, it was likely that reaction (4) also took place in the milling process.

As it was shown in a previous report [14], the hydrogen absorption kinetics of the nano-phase composite was better than that of cast single phase MmNi<sub>5-x</sub>M<sub>x</sub> alloy. It was also noted, for the nano-phase composite alloy, that Mg participated hydrogen absorption in some way at room temperature, while it is known that Mg can hardly absorb hydrogen at room temperature. The results obtained by microstructure analysis in this work give some hints for the previous results on hydrogen absorption properties of the nano-phase composite. It can be realized, at least, that the following aspects are related to the hydrogen absorption properties of the nano-phase composite. The first is that part of Mg in the composite has formed Mm<sub>2</sub>Mg<sub>17</sub> and Mg<sub>2</sub>Ni by reaction with MmNi<sub>5</sub>. The hydriding kinetics of Mm<sub>2</sub>Mg<sub>17</sub> and Mg<sub>2</sub>Ni phase are better than that of Mg. Second, the alloys obtained are nano-phase composite. There are high density of interphases and crystal defects, which are beneficial to the hydriding reaction. Besides, the

presence of nano-sized  $\text{MmNi}_5$  phase can act as catalyst to speed up hydrogenation kinetics. In fact, the fitting of kinetic curve of the nano-phase composite shows that an auto-catalytic reaction mechanism of hydriding process [23]. In recently, improvement of hydrogen sorption kinetics by forming nanocomposite structure has been reported. For examples,  $\text{MgH}_2$ -(V,Nb) nanocomposite shows very fast hydrogen sorption kinetics [24]. By forming Pd/Mg/Pd multi-layer film, the hydrogenation temperature of Mg can be lowered to 373 K [25]. Therefore, it is a potential way to improve the hydriding kinetics of Mg-base alloy by milling Mg with other hydrogen storage alloys to form nano-phase composite.

#### 4. Summary

In the present work the microstructure characteristics of  $\text{MmNi}_{5-x}\text{M}_x$ -Mg composite hydrogen storage alloys, synthesized by mechanical alloying, have been investigated by SEM, TEM and X-ray diffraction analysis. It has been found that composite particles were formed by high energy ball milling. Meanwhile,  $\text{Mm}_2\text{Mg}_{17}$  phase was formed as the milling proceeded, which indicated the occurrence of solid state reaction between  $\text{MmNi}_{5-x}\text{M}_x$  and Mg. Accompanying the formation of  $\text{Mm}_2\text{Mg}_{17}$  phase, lattice constant of  $\text{MmM}_5$  phase decreased. It has also been found that  $\text{Mg}_2\text{Ni}$  phase was formed when the milled powder was annealed at 673 K while no  $\text{Mg}_2\text{Ni}$  phase was found in the annealed sample without prior MA. This indicated that  $\text{Mg}_2\text{Ni}$  phase, in the form of amorphous, was probably formed in MA process. In order to understand the reaction took place in milling process, the reaction enthalpy of possible reactions forming  $\text{Mm}_2\text{Mg}_{17}$  phase was estimated using Miedema's model. Based on the results of experiment and enthalpy calculation, two reactions were conjectured to be responsible for the formation of  $\text{Mm}_2\text{Mg}_{17}$  in MA of Mg and  $\text{MmM}_5$ . TEM and X-ray diffraction analysis proved that all the phases obtained after MA were homogeneously distributed and their grain size was about 10–20 nanometer. In this sense, the composite obtained was not simply a mixture of Mg and  $\text{MmNi}_{5-x}\text{M}_x$  but a nano-phase composite constituted of Mg,  $\text{MmNi}_{5-x}\text{M}_x$ ,  $\text{Mm}_2\text{Mg}_{17}$  and  $\text{Mg}_2\text{Ni}$  phases.

#### Acknowledgment

This work was supported by National Natural Science Foundation under contract No. 59925102, 50071022, 50131040. The work described in this paper was

partially supported by a grant from City University of Hong Kong (Project No. 7001088).

#### References

1. H. GLEITER, *Acta Materialia* **48** (2000) 1.
2. T. MUTSCHELE and R. KIRCHHEIM, *Scr. Metall.* **21** (1987) 1101.
3. L. ZALUSKI, A. ZALUSKA and J. O. STROM-OLSEN, *J. Alloy & Compounds* **253/254** (1997) 70.
4. G. LIANG, E. WANG and S. FANG, *ibid.* **223** (1995) 111.
5. R. A. ANDRIEVSKI, B. P. TARASOV, I. I. KORBOV, N. G. MOZGNA and S. P. SHILKIN, *Int. J. Hydrogen Energy* **21** (1996) 949.
6. S. ORIMO, H. FUJI and K. IKEDA, *Acta Materialia* **45** (1997) 331.
7. H. FUJII, S. ORIMO and K. IKEDA, *J. Alloys and Compound* **253/254** (1997) 80.
8. H. FUJII, S. ORIMO and K. YAMAMOTO, *J. Less-Common Metals* **175** (1990) 243.
9. Z. YE, L. C. ERICKSON and B. HJORVARSSON, *J. Alloys & Compounds* **209** (1994) 117.
10. H. NAGAI, H. TOMIZAWA and T. OGASAWARA, *J. Less-Common Metals* **157** (1990) 15.
11. K. J. GROSS, P. SPATZ, A. ZUTTEL and L. SCHLAPBACH, *J. Alloys & Compounds* **261** (1997) 276.
12. L. ZALUSKI, A. ZALUSKA, P. TESSIER, J. O. STROM-OLSEN and R. SCHULZ R, *ibid.* **227** (1995) 53.
13. G. LIANG, S. BOILY, J. HUOT, A. VAN NESTE and R. SCHULZ, *ibid.* **268** (1998) 302.
14. M. ZHU, W. H. ZHU, Y. GAO, X. Z. CHE and J. H. AHN, *Mater. Sci. & Eng. A* **286** (2000) 130.
15. J. DING, W. F. MIAO, P. G. MCCORMICK and R. STREET, *Appl. Phys. Lett.* **67**(25) (1995) 3804.
16. H. X. SUI, M. ZHU, G. B. LI and D. Z. YANG, *J. Appl. Phys.* **71** (1992) 2945.
17. J. S. BENJAMIN, *Metall. Trans.* **1** (1970) 2943.
18. H. P. KLUG and L. ALEXANDER, "X-ray Diffraction Procedures for Polycrystalline and Amorphous Materials," 2nd ed. (Wiley, New York, 1974).
19. S. LI, K. WANG, L. Z. SUN and Z. G. WANG, *Scr. Metall. Et Mater.* **27** (1992) 437.
20. J. J. GILMAN, *Science* **274** (1996) 65.
21. T. KOGA, M. MIZUNO and M. NAGUMO, *Mater. Sci. Enger. A* **179/180** (1994) 153.
22. F. R. DE BOER, R. BOOM, W. C. M. MATTENS, A. R. MIEDEMA and A. K. NIESSEN, "Cohesion in Metals-Transition Metal Alloys" (Elsevier Science Publishers, B. V., North-Holland, 1989).
23. M. ZHU, Y. GAO, X. Z. CHE, Y. Q. YANG and C. Y. CHUNG, *J. Alloys & Compounds* **330–332** (2002) 708.
24. J. HOOUT, J. F. PELLETIER, G. LIANG, M. SUTTON and R. SCHULTZ, *ibid.* **330–332** (2002) 727.
25. K. HIGUCHI, K. YAMAMOTO, H. KAJIOKA, K. TOIYAMA, M. HONDA, S. ORIMO and H. FUJII, *ibid.* **330–332** (2002) 526.

Received 9 January 2002

and accepted 5 March 2003